



Review

# Recent Breakthroughs and Advancements in NO<sub>x</sub> and SO<sub>x</sub> Reduction Using Nanomaterials-Based Technologies: A State-of-the-Art Review

Moazzam Ali <sup>1,†</sup> , Ijaz Hussain <sup>2,†</sup>, Irfan Mehmud <sup>3</sup>, Muhammad Umair <sup>4</sup> , Sukai Hu <sup>4</sup> and Hafiz Muhammad Adeel Sharif <sup>4,\*</sup>

<sup>1</sup> Centre of Excellence in Solid State Physics, University of the Punjab, Lahore 05422, Pakistan; mak.ssp@yahoo.com

<sup>2</sup> Key Laboratory of the Ministry of Education for Advanced Catalysis Materials, Institute of Physical Chemistry, Zhejiang Normal University, Jinhua 321004, China; ijaz9292@gmail.com

<sup>3</sup> Health Science Center, Shenzhen University, Shenzhen 518060, China; Irfan\_Mehmud\_1984@hotmail.com

<sup>4</sup> College of Chemistry and Environmental Engineering, Shenzhen University, Shenzhen 518060, China; umair\_uaf@hotmail.com (M.U.); 2110223076@email.szu.edu.cn (S.H.)

\* Correspondence: hmadeelcmc@hotmail.com

† Moazzam Ali and Ijaz Hussain contributed equally to this work.

**Abstract:** Nitrogen and sulphur oxides (NO<sub>x</sub>, SO<sub>x</sub>) have become a global issue in recent years due to the fastest industrialization and urbanization. Numerous techniques are used to treat the harmful exhaust emissions, including dry, traditional wet and hybrid wet-scrubbing techniques. However, several difficulties, including high-energy requirement, limited scrubbing-liquid regeneration, formation of secondary pollutants and low efficiency, limit their industrial utilization. Regardless, the hybrid wet-scrubbing technology is gaining popularity due to low-costs, less-energy consumption and high-efficiency removal of air pollutants. The removal/reduction of NO<sub>x</sub> and SO<sub>x</sub> from the atmosphere has been the subject of several reviews in recent years. The goal of this review article is to help scientists grasp the fundamental ideas and requirements before using it commercially. This review paper emphasizes the use of green and electron-rich donors, new breakthroughs, reducing GHG emissions, and improved NO<sub>x</sub> and SO<sub>x</sub> removal catalytic systems, including selective/non-catalytic reduction (SCR/SNCR) and other techniques (functionalization by magnetic nanoparticles; NP, etc.). It also explains that various wet-scrubbing techniques, synthesis of solid iron-oxide such as magnetic (Fe<sub>3</sub>O<sub>4</sub>) NP are receiving more interest from researchers due to the wide range of its application in numerous fields. In addition, EDTA coating on Fe<sub>3</sub>O<sub>4</sub> NP is widely used due to its high stability over a wide pH range and solid catalytic systems. As a result, the Fe<sub>3</sub>O<sub>4</sub>@EDTA-Fe catalyst is projected to be an optimal catalyst in terms of stability, synergistic efficiency, and reusability. Finally, this review paper discusses the current of a heterogeneous catalytic system for environmental remedies and sustainable approaches.

**Keywords:** NO<sub>x</sub> and SO<sub>x</sub> removal; wet-scrubbing; catalytic systems; Fe<sub>3</sub>O<sub>4</sub> nanomaterial



**Citation:** Ali, M.; Hussain, I.; Mehmud, I.; Umair, M.; Hu, S.; Sharif, H.M.A. Recent Breakthroughs and Advancements in NO<sub>x</sub> and SO<sub>x</sub> Reduction Using Nanomaterials-Based Technologies: A State-of-the-Art Review. *Nanomaterials* **2021**, *11*, 3301. <https://doi.org/10.3390/nano11123301>

Academic Editors: Gang Pan, Lei Wang and Jafar Ali

Received: 22 October 2021

Accepted: 30 November 2021

Published: 6 December 2021

**Publisher's Note:** MDPI stays neutral with regard to jurisdictional claims in published maps and institutional affiliations.



**Copyright:** © 2021 by the authors. Licensee MDPI, Basel, Switzerland. This article is an open access article distributed under the terms and conditions of the Creative Commons Attribution (CC BY) license (<https://creativecommons.org/licenses/by/4.0/>).

## 1. Introduction

To keep life simple and comfortable is a concept as old as the beginning of time and this leads to the new inventions, discoveries and forward efforts. The quest for ease and a more convenient life strives to utilize the surrounding things and convert them into useful items. The start of the things always positive and man used the available items present in the surroundings. The same concept comes from burning or combustion (burning of substance by oxygen and generating heat i.e., energy accompanying flame i.e., light). This burning of fossil fuels has been observed from the earliest times and all people get advantages in different ways. Every new civilization improves it to meet their needs. Although the use of fossil fuels has created new customs, the overuse of combustion and its adverse effects

cannot be denied [1,2]. Although, the energy obtained through combustion is very useful, it leaves adverse effect on marine life, ecosystem, human health and environment [3,4].

The rapid, cheap, and unlimited energy demands are the major reasons for producing electricity via combustion or fossil fuel. This results in an over demand for cheap energy and combustion of fossil-fuel eliminating toxic gases such as nitrogen oxides ( $\text{NO}_x$ ), sulfur dioxide/trioxide ( $\text{SO}_x$ ) and carbon monoxide (CO), which are rapidly increasing air-pollution [5]. The total contribution by fossil fuels for electricity production is shown in Figure 1 [6–8]. The basic reason is that fossil fuel combustion for electricity production is the major anthropogenic source of atmospheric pollutants. Therefore, coal is the most significant source of electrical energy, and it is projected to increase by a particular ratio each year for the next 25 years. Coal is cheap and readily available everywhere, and it is still believed that coal will be the considerable source for the next two decades for the production of power [9–11].  $\text{NO}_x$  and  $\text{SO}_x$  containing flue gases were also released by the combustion of fuel and gas, but the concentration of these gases in coal-burning was roughly 2 to 3 times higher than that in gas burning [12]. Based on this calculation approximately 40 to 50% of the electrical energy of the world is being generated by coal-fired power plants [13]. Previously, several review studies were conducted to cover significant features of  $\text{NO}_x$  and  $\text{SO}_x$  elimination techniques, including wet scrubbing, SCR/SNCR etc. However, there is still a gap in the literature for a state-of-the-art review paper focused on a combination of using green and electron-rich donors, new breakthroughs, reducing GHG emissions, and improved  $\text{NO}_x$  and  $\text{SO}_x$  removal catalytic systems, including selective/non-catalytic reduction (SCR/SNCR) and other techniques (functionalization by magnetic nanoparticles; NP, etc.) [14].

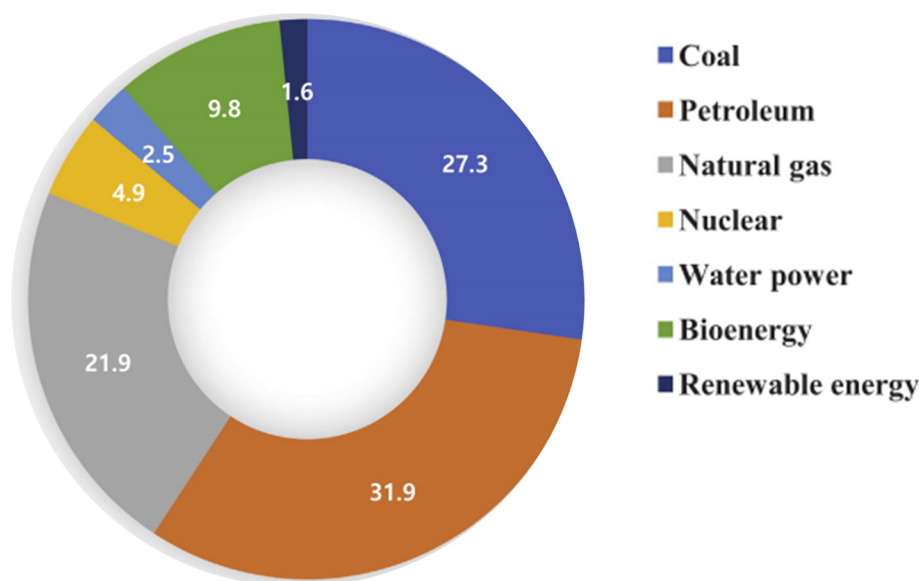


**Figure 1.** World demand forecast by primary energy source. Adapted with permission from [6]. Copyright, 2019 Elsevier.

## 2. $\text{NO}_x$ and $\text{SO}_x$ Emission from Combustion

Industrialization and urbanization push the environment more adversely by producing more than 90% of  $\text{NO}_x$  because of fuel combustion. Furthermore, the pollutants from various sources such as unlimited combustion of industries, coal-fired power plants, on-road vehicles, aviation transport, gas and fuel refineries combustion exacerbate the situation daily. These sources left the worse effect on the atmospheric equilibrium by the emission of acidic gases ( $\text{NO}_x$ ,  $\text{SO}_x$ ) and particulate matter (PM), which are causing many negative impacts on environment, as well as for health [15,16]. The short overview of primary pollutants ( $\text{NO}_x$ ,  $\text{SO}_x$ ) is shown in Table 1 [17]. The infinite industrial exhaust in the lower atmosphere needs controlled for the sustainability of environmental balance by

treating the toxic gases. Recently, various stringent laws and regulations have been developed worldwide to reduce the peril influence of toxic gases, especially by anthropogenic sources. The general trend for  $\text{NO}_x$  and  $\text{SO}_x$  emissions from power plants can be found such as in this Equation (1) [12].

$$\text{Gas-emission} > \text{oil-emission} > \text{coal-emission} \quad (1)$$

**Table 1.** Details of  $\text{NO}_x$  and  $\text{SO}_2$  combustion pollutants.

Name	Formula	Characteristic	Source	When and Where	Health Problems	Atmospheric Problems
Sulphur dioxide	$\text{SO}_2$	Colour less	Coal plants, vehicles, industries	London 1952, Beijing, China 1985	Damages Lungs tissue, asthma	Smog, ozone formation, acid rain
Nitric oxide	$\text{NO}$	Colorless	Coal plants, vehicles, industries	Los Angeles 1940, Beijing, China 1985	Chronic respiratory, visibility, lungs damage, breast cancer, asthma attacks	Smog, ozone formation, acid rain, secondary pollutants
Nitrogen dioxides	$\text{NO}_2$	Reddish-brown	Combustion, nitric acid plants			

### 2.1. Adverse Effect of $\text{NO}_x$

The pollution is chronic and becomes acute after entering the human body. The most common and fundamental way in contact with air respiration and ingestion and skin contact also risk [18]. Even though the harmful effect of only  $\text{NO}_x$  is not irrevocable and thought to be toxic. This gas in the air and oxygen combination also generates many other secondary pollutants and forms photochemical smog [19,20]. For example, the  $\text{NO}$  is less harmful than  $\text{NO}_2$  and affects the eyes and throat. The more common and stable nitrogen oxides are given in Table 2 with their characteristics. As a result, the number of contaminants released into the atmosphere increases, and people are affected by blends and combinations of pollutants that may lead to more severe health issues [21].

**Table 2.** The most common existing nitrogen oxides and their physical properties of these oxides are given. Adapted with permission from [22]. Copyright, 2010 Elsevier.

Nitrogen Oxides	Color	Solubility ( $\text{g}\cdot\text{dm}^{-3}$ ) [23]	State	Density ( $\text{g}\cdot\text{dm}^{-3}$ )
$\text{NO}$	Colorless	0.032	Gas	1.3402
$\text{N}_2\text{O}$	Colorless	0.111	Gas	1.8
$\text{NO}_2$	Red-brown	213.0	Gas	3.4
$\text{N}_2\text{O}_4$	Transparent	213.0	Liquid	1492.7 (273 K)
$\text{N}_2\text{O}_5$	White	500.0	Solid	20,508 K

### 2.2. $\text{NO}_x$ Treatment Techniques

To meet the requirement of environmental protection organizations, a number of ways have been developed and executed on the individual industrial level for the treatment of  $\text{NO}_x$ ,  $\text{SO}_2$ . Some techniques are used to decrease  $\text{NO}_x$  production during combustion, on the other hand, many ways are also applied to reduce the post-combustion. The overview of currently used abatement technologies is shown in Figure 2. The treatments include dry sorbent injection (DSI), selective noncatalytic reduction (SNCR), wet flue gas desulfurization (FGD), and selective catalytic reduction (SCR) [24,25]. For the treatment of  $\text{NO}_x$  and  $\text{SO}_2$ , FGD and SCR are the two most commonly employed technologies.

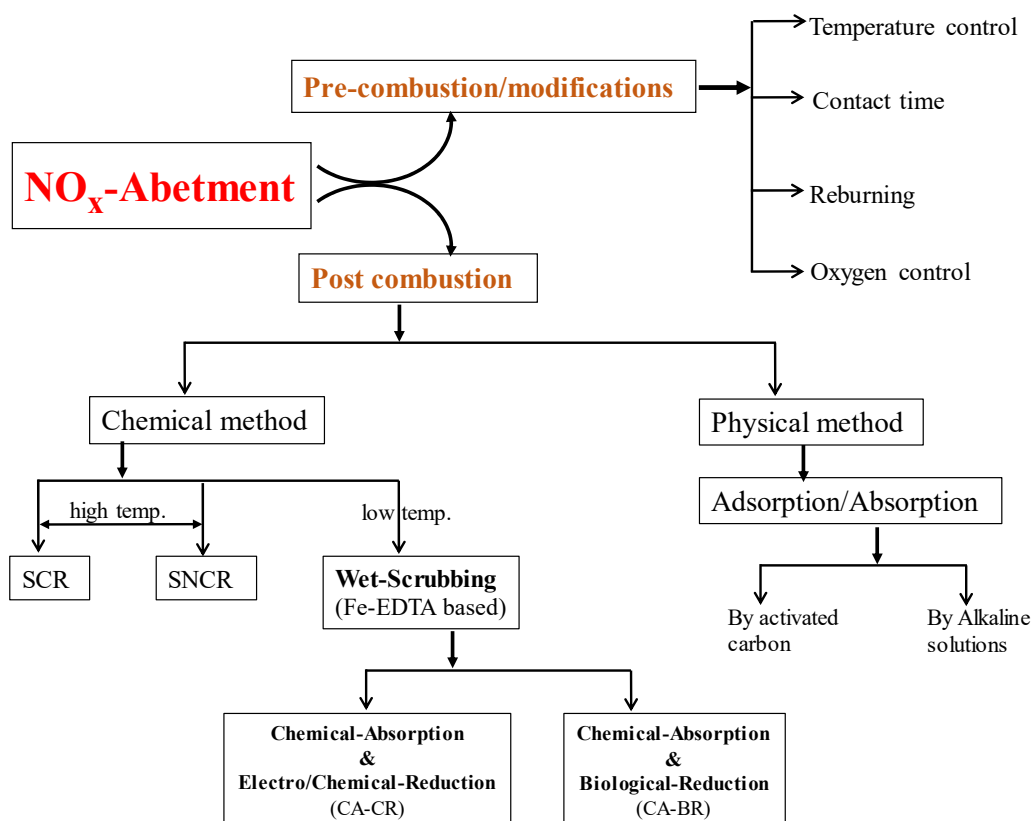
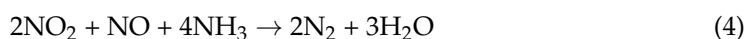
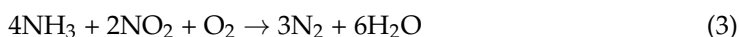
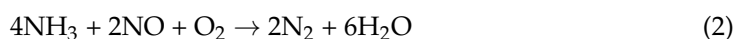


**Figure 2.** General overview of NO<sub>x</sub> abatement systems by pre combustion and post combustion techniques, which further divided into specific methods based on operations.

### 2.2.1. Selective Catalytic Reduction (SCR)

SCR is the most widely executed technique all over the world for flue gas and fuel combustion treatment on industrial and large-scale NO<sub>x</sub> emission. This technique was introduced by Japan about 45 years ago and later also implemented in USA, Germany and many other European countries. In this technique, ammonia and air are mixed with NO gas in the presence of a catalyst (metallic-oxides), and under high temperature (250–600 °C), NO reduced into N<sub>2</sub> and water ash are shown here [26,27].

Usually, the reduction efficiency of NO<sub>x</sub> depends upon the addition of ammonia for a specific amount of NO<sub>x</sub> (NO and NO<sub>2</sub>) as shown following, Equations (2)–(4).



Because of its high acid strength ( $\text{H}^+ \leq -5.6$ ) and remarkable Lewis and Brönsted acidity, Nb<sub>2</sub>O<sub>5</sub> is the most extensively used catalyst of all [28]. The doping of Nb<sub>2</sub>O<sub>5</sub> to Fe<sub>2</sub>O<sub>3</sub> catalyst for the NH<sub>3</sub>-SCR reaction was initially described in 1985, and it is still in use today [29]. Although this phenomenon was discovered, the promotion mechanism was lost due to the limited characteristic procedures available at the time. According to a recent study, Ma et al. discovered that excellent SCR performance is achieved through using a Nb promoted CeZrO<sub>x</sub> catalyst, which demonstrated high catalytic activity and N<sub>2</sub> selectivity over a wide temperature range of 190–460 °C [30]. Mosrati et al. revealed that after Nb doping, a Ce/Ti catalyst displayed high activity and N<sub>2</sub> selectivity, and Ce dispersion and strong acidity were essential factors in the catalyst's high activity [31]. Nb addition can boost the catalyst's anti-heavy metal poisoning activity as well as catalytic activity. Li et al.

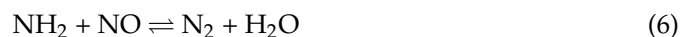
reported that modifying Mn/TiO<sub>2</sub> catalysts with Nb increases Zn resistance [32]. Adding Nb to MnO<sub>x</sub> (Mn-Nb mixed oxide catalysts) increases NO conversion and N<sub>2</sub> selectivity due to increased Bronsted acidity and combining MnO<sub>x</sub> and NbO<sub>x</sub> [33]. In spite of the fact that the Nb modification boosted the acidity of the catalyst, it also reduced its reducibility, resulting in a synergistic relationship between acidity and reducibility in terms of the catalyst's catalytic activity. In other words, the acidity and reducibility work together to enhance the catalytic activity [32].

### 2.2.2. Selective Noncatalytic Reduction (SNCR)

It is possible to reduce NO by using a reagent, often ammonia or urea, at temperatures between 850 °C and 1175 °C using the SNCR approach [34]. This technique was also introduced by Japan in the late of 1970s [9,35]. In this experiment, the reagent, ammonia, combines with hydroxyl radicals (OH) to generate an amidogen radical (–NH<sub>2</sub>), which is as follows:



when exposed to NO, this radical is selectively reactive and is most commonly involved in the following reactions:

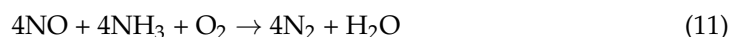


The importance of reaction (8) can be attributed to the fact that it is a chain branching reaction that regenerates OH radicals required by the chain propagation reaction (5). However, a further reaction occurs with the NNH radical:



More hydroxyl radicals are generated because of a chain reaction involving the H atom.

However, for normal operation of this technique the stoichiometric ration is about 4-times as compared to SCR for NO<sub>x</sub> removal-reduction as shown in the following chemical reactions Equations (10) and (11) [36].



In stationary combustion systems, ammonium sulphate is being investigated as an addition for the simultaneous control of NO<sub>x</sub> (via SNCR) and deposition and corrosion and sulfation of alkali chlorides). According to Kristian et al., ammonium sulphate SNCR performance was assessed in a laboratory-scale flow reactor. NO reductions up to 95% were achieved at temperature range 1025–1075 °C, while using 5 and 10 w% solutions of aqueous ammonium sulphate, respectively, corresponding to ammonium sulphate/NO ratios over 1 [37]. According to reported literature, sulphur from ammonium sulphate is primarily emitted as SO<sub>3</sub>, even though SO<sub>2</sub> is identified in high concentrations at very high temperature (e.g., over 1000 °C). There was evidence that adding KCl to the SNCR process promoted the reaction at lower temperatures, resulting in an additional 50 degrees Celsius of reduction potential. The high degree of KCl sulfation at or below 1000 °C was enabled by ammonium sulphate, suggesting the possibility of utilizing ammonium sulphate in full-scale combustion facilities to reduce NO<sub>x</sub> and corrosion simultaneously. The experiments were analyzed in terms of a thorough kinetic model that was used. Even though the NO reduction at the optimum was significantly underestimated, the model accurately reproduced the SNCR experiments performed using ammonium sulphate. In addition, KCl sulfation was effectively documented; the enhancing effect of KCl on SNCR with ammonium sulphate was grossly overestimated. Possible explanations for this disparity were considered [22,38].

### 2.2.3. Limitations of SCR and SNCR

However, the aforementioned methods are decent but still have limitations such as high temperature 700–1100 °C, less efficient for reduction-removal for SNCR, intrinsic use of additional chemicals, high cost, use of surplus freshwater, land area for FGD, and high temperature 300–750 °C, deactivation of catalysts and control of secondary pollutants such as ammonia (NH<sub>3</sub>) and hydrocarbons for SCR [39,40]. Another major drawback of this technology is that at high temperature for NH<sub>3</sub> and NO gas mixture, the NH<sub>3</sub> becomes oxidized at >400 °C. The oxidation of NH<sub>3</sub> inhibits the further reduction or transformation of NO, which is not acceptable [41]. The universal law is that at high temperatures, the molecules of substances produce more energy, similarly, NH<sub>3</sub> slips from the reaction chamber and escape into the atmosphere [35]. These parameters limit the applicability for execution on the industrial level. The low temperature and environmentally friendly techniques are highly appreciated.

### 2.2.4. Common Solid Adsorbent Materials

Mostly post-combustion techniques are practiced due to the efficient reduction of NO<sub>x</sub> and the objective of this work focuses on this method. Some other techniques also have been accessed, which are based on physical absorption of NO, including metal–organic frameworks (MOFs) such as (MIL: Materials of Institute Lavoisier) MIL-88A(Fe), MIL-96(Pt), MIL-100(Fe, Mn) and MIF-74(Co, Mn), activated carbon (AC), lime (CaSO<sub>4</sub>), zeolites and direct metal oxides. However, due to low efficiency, deactivation of materials, mist flue gas and selectivity either for NO or SO<sub>2</sub> also inhibit the large-scale applications of these techniques [42,43]. Moreover, MOFs and zeolites are famous for their highest absorption capacity due to their large surface area and highest active sites for scavenging. Hence, the MOF's materials are also extensively used for storage, transportation of gases and specially for NO storage, only MOFs were being chosen. To avoid the side effects (e.g., redox reaction of NO<sub>x</sub>), it is stored in special non-reacting cages made of MOFs and only released at the time of use [43,44].

MgO-organic component materials were synthesized using glucose and polyvinylpyrrolidone as raw materials in a one-step hydrothermal process. When combined with NO<sub>x</sub> removal, the material is utilized to increase the efficiency of SO<sub>2</sub> removal while simultaneously decreasing the competitive adsorption of both. It was determined if MgO-organic component/pure MgO/MgO (PVP modified)/MgO (glucose modified) improved the adsorption of SO<sub>2</sub> and NO<sub>x</sub> in the simulated coal-fired flue gas in the trials, and the comparison of the test findings was made. The MgO-organic components SO<sub>2</sub> dynamic adsorption capacity was 0.3627 mmol/g, while NO<sub>x</sub> was 0.2176 mmol/g, and the adsorption breakthrough time (time taken when the NO<sub>x</sub> removal rate was 50%) was as long as 60 min (total flow rate of simulated flue gas is 200 mL/min, space velocity is 24,000 h<sup>-1</sup>, the reaction temperature is 100 °C, the concentration of SO<sub>2</sub> and NO<sub>x</sub> is 50% [45].

## 3. Low Temperature-Based Abatement Technique

### 3.1. Metal Ligand Absorption

Researchers and environmentalists have been working on alternative solutions to the concerns listed above and explored various approaches. Another critical thing to be discussed here is the NO solubility problem in water. Some other toxic gases such as CO<sub>2</sub> and SO<sub>2</sub> are easily treated via the alkali absorption method [46,47]. Since the solubility problem NO can be treated such as other gases, it required some combined or integrated system applied for NO reduction [48]. This solubility problem indicated the NO<sub>x</sub> removal would be easier if chemical modifications were used for its absorption and reduction. Many ways came to notice, but most practice has been undertaken by wet scrubbing using Fe-EDTA. There are several reasons for considering flue gas treatment and reduction techniques, which are discussed herein. The MnO<sub>x</sub>/CNT<sub>s</sub> catalysts were found to have unusual SCR activity at low temperatures when they were first synthesized. When using the optimal 1.2 percent MnO<sub>x</sub>/CNT<sub>s</sub> catalyst at 80–180 °C, the NO conversion ranged between

57.4 and 89.2 percent. This occurred from the use of amorphous  $\text{MnO}_x$  catalysts, which have a higher ratio of  $\text{Mn}^{4+}$  to  $\text{Mn}^{3+}$  and  $\text{O}_S$  to  $(\text{O}_S + \text{O}_L)$  than the crystalline  $\text{MnO}_x$  catalysts [49]. By impregnation and in situ deposition methods, the same Ce/Mn molar ratio was achieved in the preparation of Ce (1.0) Mn/TiO<sub>2</sub> catalysts. In comparison to the impregnation-prepared Ce(1.0)Mn/TiO<sub>2</sub>-IP catalyst, the in situ deposition-prepared Ce(1.0)Mn/TiO<sub>2</sub>-SP catalyst demonstrated superior catalytic activity throughout a wide temperature range (150–300 °C) and at high-gas hourly-spaced velocities ranging from 10,500 to 27,000 h<sup>-1</sup>. Furthermore, the Ce(1.0)Mn/TiO<sub>2</sub>-SP catalyst produced by the in situ deposition approach has superior sulphur resistance to the Ce(1.0)Mn/TiO<sub>2</sub>-IP catalyst [50,51]. By using the citric acid–ethanol dispersion method, a variety of Gadolinium (Gd)-modified  $\text{MnO}_x$ /ZSM-5 catalysts were produced and assessed using a low-temperature  $\text{NH}_3$ -SCR reaction. Of them, the GdMn/Z-0.3 catalyst, which had a molar ratio of 0.3 for Gd to Mn, had the maximum catalytic activity, and it was capable of achieving a 100 percent NO conversion in the temperature range of 120–240 degrees Celsius. Furthermore, when tested in the presence of 100 ppm  $\text{SO}_2$ , GdMn/Z-0.3 demonstrated superior  $\text{SO}_2$  resistance when compared to Mn/Z. It was demonstrated that such catalytic efficacy was primarily driven by surface chemisorbed oxygen species, a wide surface area, an abundance of  $\text{Mn}^{4+}$  and, a proper acidity and reducibility, and the of the catalyst, among other factors [52].

### 3.2. Metal Ligand Stability

Among transition metal chelating complexes, Fe-EDTA is the most favorable and stable chelate against the long-range of pH. Comparison for the metal chelate system are also shown in Figure 3. On top of that, ferrous (Fe(II)) has the great affinity towards the NO compared to other d-block elements. By taking advantage of this Fe-EDTA stability and greatest affinity, it has been used for NO<sub>x</sub> removal from flue gas. Another advantage of this process (wet scrubbing) is the simultaneous removal of NO<sub>x</sub> and SO<sub>2</sub> under ambient conditions. Moreover, the NO<sub>x</sub> interaction with Fe(II) is direct chemically binding and forms a very stable bond among other transition metals [12,53].

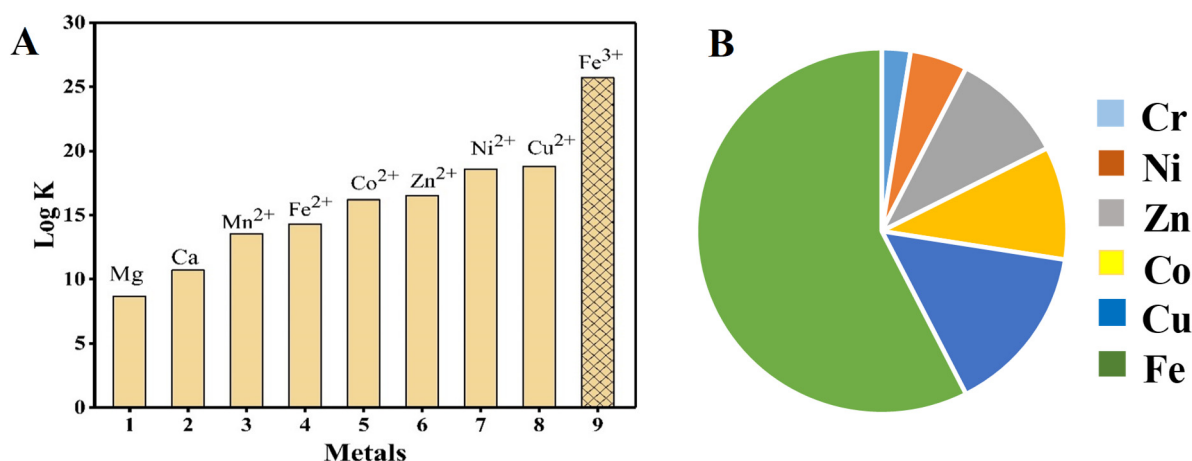


**Figure 3.** (A) Relative stability of Fe-EDTA with other metals, (B) relative NO gas and transition metal interactions.

### 3.3. Principle of Gas Absorption

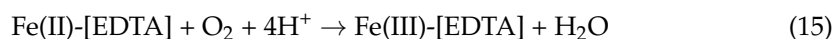
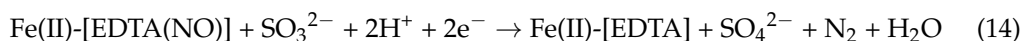
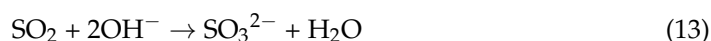
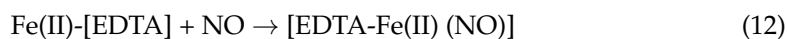
Basically, this concept is composed of two steps, (i) Fe-EDTA solution absorbs NO<sub>x</sub> molecule via making metal-nitrosyl-complex and then (ii) this NO<sub>x</sub> reduced into N<sub>2</sub>O, N<sub>2</sub> and N-S compounds by utilizing the SO<sub>2</sub>, which is a compulsory part of flue gas. This SO<sub>2</sub> transformed into SO<sub>3</sub><sup>2-</sup> by alkali absorption and reduced NO<sub>x</sub> by converting itself into SO<sub>4</sub><sup>2-</sup> ions. During the reduction of NO<sub>x</sub>, the scrubber (Fe-EDTA) also regenerated irrespective the valence form of iron, Fe(II) or Fe(III). As Fe(III) is more stable due to more stability than Fe(II), it cannot be restored without the help of the electron donor externally.

The number of electron donors used to reduce Fe(III) back to Fe(II) depends upon the source, condition and more important the NO<sub>x</sub> reduction process.

#### 4. Wet Scrubbing

##### 4.1. Chemically Absorption by Metal-Ligand System

Several studies have demonstrated that wet scrubbing procedures are highly efficient, do not require intrinsic chemicals and are regenerable, requiring no additional fresh water or solution. This approach obtains EDTA-Fe(II) for chemical NO absorption by forming a metal-nitrosyl-complex, then, subsequently, reduced either by externally added sulphite solutions (SO<sub>3</sub><sup>2-</sup>) or by transforming SO<sub>2</sub> into SO<sub>3</sub><sup>2-</sup> ions through alkali absorption. The reductant may be activated carbon (AC) or an electrochemical system to provide electron for NO<sub>x</sub> reduction and Fe-EDTA regeneration. As this reduction has been performed chemically so it is famous by name de-NO<sub>x</sub>/chem-de-NO<sub>x</sub>. Although wet scrubbing is good enough but due to oxygen contents which is a compulsory part of flue gas, make scrubber inactive by oxidation of EDTA-Fe(II) into EDTA-Fe(III) as shown in the followings Equations [54,55].



##### 4.2. NO<sub>x</sub> Removal by Different Techniques

In the same way, there is also another analog technique of chemical wet scrubbing, i.e., bio-de-NO<sub>x</sub>. In this technique, the absorption step is similar to chem-de-NO<sub>x</sub>, but some biological reduction methods used the transformation of NO<sub>x</sub> regeneration of Fe-EDTA. The later step is carried out in the presence of microorganisms or bacteria under typical conditions; hence, it is called bio-de-NO<sub>x</sub>. The schematic diagram of bio-de-NO<sub>x</sub> and chem-de-NO<sub>x</sub> is shown in Figure 4. The difference in reduction or source of electron donor varies in both processes [56,57].

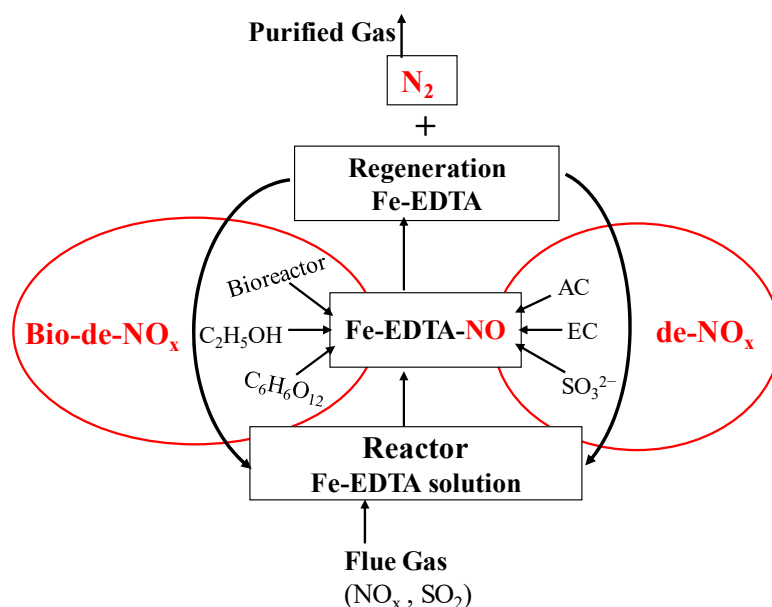


**Figure 4.** Schematic diagram for de-NO<sub>x</sub> and bio-de-NO<sub>x</sub>.

The absorption of NO<sub>x</sub> for Fe-EDTA-based wet scrubbing is the same but reduction after making metal-nitrosyl-complex is different. The reduction in de-NO<sub>x</sub>/chem-de-NO<sub>x</sub>



is also carried out chemically by AC, sulphite solution; hence, it is known as chemical absorption and chemical reduction (CA-CR). In the same way, chemical absorption is integrated with the biological approach so that it is named a bio-de-NO<sub>x</sub> system. In this integrated system, the reduction is carried out biologically via bacteria or microorganism by using glucose, ethanol, and chemical absorption and biological reduction (CA-BR). Both techniques CA-CR and CA-BR are accomplished at low temperature or mostly at room temperature, which is more suitable and cost-effective. As these processes are relatively similar, the problem (regeneration, efficiency, sustainability) of these technologies is also similar to some extent. Our newly published review paper on hybrid wet-scrubbing approaches for the removal of NO<sub>x</sub> and SO<sub>2</sub> can be referred to for further information [2,35].

## 5. Challenges of Wet Scrubbing Method

### 5.1. Regeneration of Fe-EDTA

The oxidized (EDTA-Fe(III)) fails to bind the NO from flue gas due to the stability of ferric (Fe(III)) ions [58]. Reducing Fe(III) into ferrous (Fe(II)) can be accomplished in many ways but the preparation of reducing agents and constantly feeding-up reactors is not highly appreciated. To more sustainable and promising method, the system should be self-generated, i.e., it can be regenerate when used in operation, and the regeneration of Fe(II) is a pre-requisite of this technique. Therefore, the regeneration of Fe(II)-EDTA is not an easy task, so we have added some external reductants, which can assist the regeneration of Fe(II) from Fe(III) [59]. These externally added reductants help reduce the NO into N<sub>2</sub> and regenerate Fe(II) after completing the cycle, as shown in Figure 5. Many researchers used a number of reductants to restore the Fe(II) back for NO absorption; some examples of reductants are also given in Table 3.

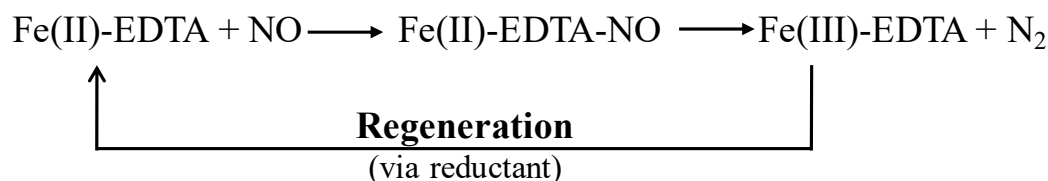


**Figure 5.** NO absorption, reduction and regeneration of Fe(II)-EDTA by external reductant.

**Table 3.** The commonly used electron donor for regeneration of Fe-EDTA (ferric to ferrous) by different people during NO<sub>x</sub> reduction via wet scrubbing (chemical reduction and biological reduction).

Chemical Reduction			Biological Reduction		
Reductants	Year	Ref.	Reductants	Year	Ref.
Na <sub>2</sub> SO <sub>3</sub>	1984	[60]	Ethanol	1999	[61]
SO <sub>3</sub> <sup>2-</sup>	1980	[62]	Acetate	2003	[63]
HSO <sub>3</sub> <sup>2-</sup>	1990	[55]	Glucose	2007	[64]
Polyphenolic compounds	1991	[59]	Gallic acid pyrogallol and tannic acid	1991	[65]
Hydrazine	1994	[1]			
Na <sub>2</sub> S <sub>2</sub> O <sub>4</sub>	2005	[66]			
Na <sub>2</sub> S	2006	[67]			

### 5.2. Secondary Pollutant

Although this system has many advantages such as it operates at low temperature, does not need extra intrinsic chemicals and scrubber solution is also regenerated, paradoxically, this system still has drawback by generating the secondary pollutant, nitrous oxide (N<sub>2</sub>O). This N<sub>2</sub>O is generated as an intermediate or by-products with N<sub>2</sub> during NO<sub>x</sub> reduction as shown in Figure 6 [55]. On the top of that the production of secondary pollutants, nitrous oxide (N<sub>2</sub>O) more water-soluble and separation from solution mixture is not easy. The main reason is the optimize pH for NO absorption and separation of

$N_2O$  is different, hence, to grab the  $N_2O$  almost impossible. The emission of this  $N_2O$  is released by tail gas or treated gas, which is very secondary pollutant and very stable in the atmosphere.

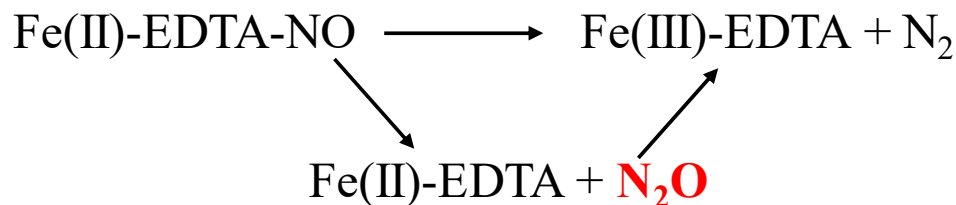


**Figure 6.** Reduction of NO via formation of  $N_2O$  as an intermediate.

### 6. Drawback of Wet Scrubbing

The absorption and reduction take place under the same conditions (specially pH) so that the recovery of  $N_2O$  is not easy by this technique. Another critical problem is that the solubility of  $N_2O$  in water is 5-fold than that of NO gas, so the separation of  $N_2O$  is not easy [68]. It is one of the stable greenhouse gasses (GHG) and creates a number of problems after emission from  $NO_x$  treatment plant.  $N_2O$  takes place by tail gas, which is a very serious issue because it is one of the GHG and causes serious problems such as ozone depletion substance (ODS) [69]. The accumulation of  $N_2O$  in the atmosphere is again a critical problem that generates more N-oxides and, subsequently, causes atmospheric pollution.

### 7. Iron Oxide Nanoparticles

The retrieval of  $N_2O$  is not possible from water, i.e., a significant amount is dissolved into water and finally released with tail gas, which again leads to the problem. This problem is not due to the solution mixture, it only relates to the applied condition and specially pH, and it is the main problem of this system. This problem can be resolved if the system operates under two different conditions i.e., absorption and reduction. This could be achieved easily if we transform the nature of Fe-EDTA into a solid form or by anchoring it into metallic particles solid particles. For metallic support, the iron-oxide nanoparticles (IONP) could be an excellent choice for many reasons. Iron is an indispensable part of chemistry, and a number of solid materials, composites and other catalytic tools are used on micro- and macro-levels. In addition, the overall reported iron-oxides are 16, but there are three main groups. Obviously, these three groups are due the stability and extensive occurring on the earth crust throughout the world. These iron oxides exist naturally and these groups with examples shown in Table 4 [70].

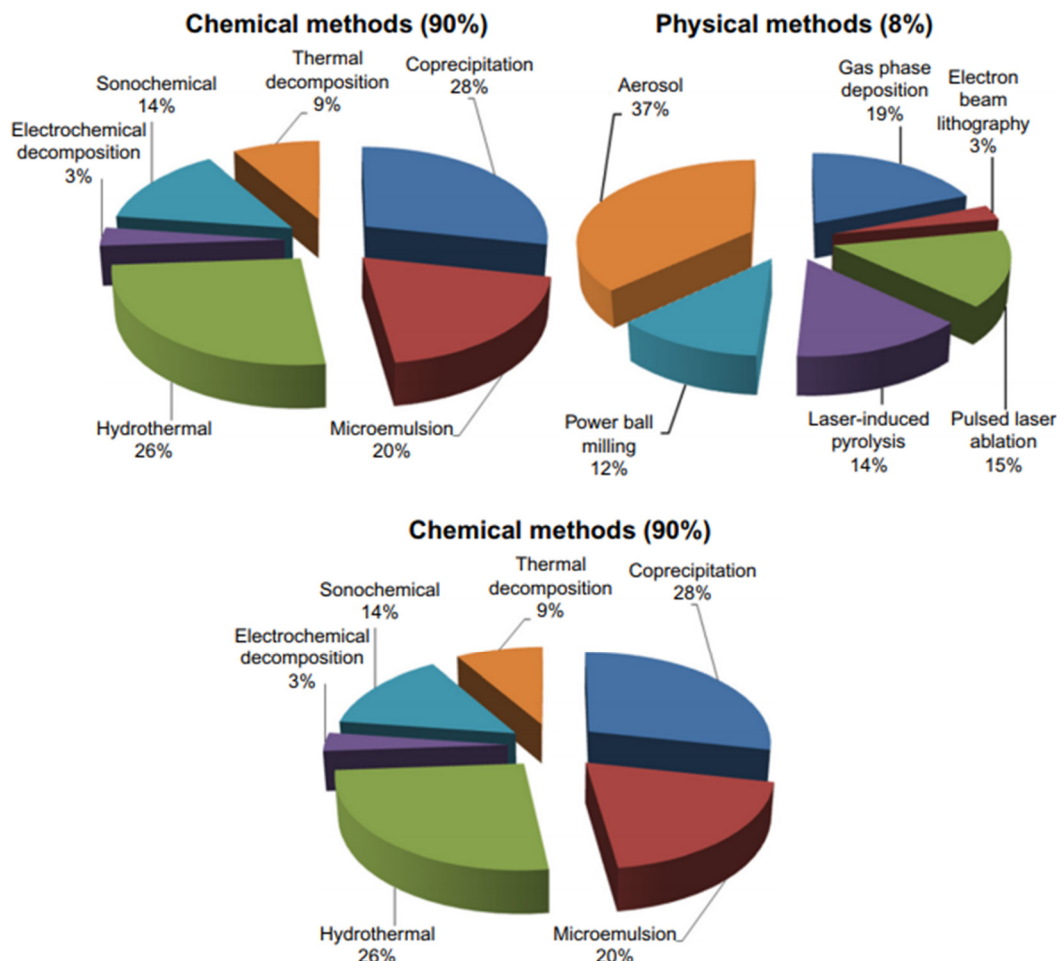
**Table 4.** Most common and major groups of Iron-oxide based on valence.

Name	Oxidation State	Examples
Ferric oxides	Fe(III)	Ferrihydrite, goethite, lepidocrocite
Ferrous oxides	Fe(II)	Fe(II)O, Fe(II)(OH) <sub>2</sub>
Mixed-valent iron oxides	Fe(III) and Fe(II)	Magnetite, green rust (GR)

#### 7.1. Synthesis of Magnetic Iron-Oxide Nanoparticles

Out of these oxides, ferric Fe(III) oxides exist abundantly due to oxygen and more stable electronic configuration. The Fe(III) oxides formed naturally into magnetite and green rust via Fe(II) conversion under specific conditions [70]. However, the magnetic compounds exist naturally and are synthesized in the laboratory. The synthesized magnetite (Fe<sub>3</sub>O<sub>4</sub>) are nano-sized super magnetic independent particles with different characteristics, structures, and its applications. There are a number of ways to synthesis these magnetic nanoparticles (NP) depending upon the characteristic application in nanoscience and nanotechnology [71,72]. Due to distinguished magnetic response, large surface area, and low

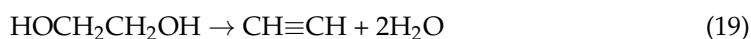
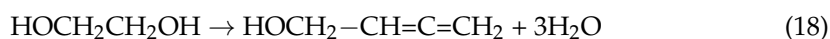
cytotoxicity, the synthesis of Fe<sub>3</sub>O<sub>4</sub> NP materials has been of hot interest in the last two decades. Therefore, several different ways have been discovered, to date, and a relative comparison of synthesis is shown in Figure 7 [73].

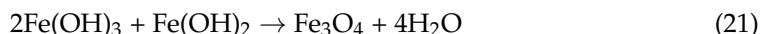
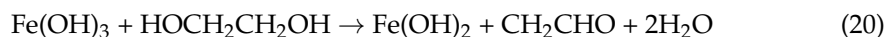


**Figure 7.** Relative comparison for the synthesis of iron oxide nanoparticles (IONP) by three different main categories that are further classified into different types based on sources and predominant principles. Adapted with permission from [73]. Copyright, 2016 Dovepress.

### 7.2. Solvothermal Synthesis

Out of these fabrication methods, the chemical method is attaining more interest and is mostly implemented due to high efficiency, low cost, simple easily adaptable and controllable [74]. Mostly chemical methods are achieved by basic iron salts, common acid-base and solvents used under easily achievable temperature and pH. The predominant techniques are different based on crystalline structure, size, and sometimes its magnetic properties [75]. The solvothermal method is more suitable for crystalline Fe<sub>3</sub>O<sub>4</sub> NP than the oxygen-free environment, which is relatively expensive with controlled particles and shape [74]. The most common chemical reactions involved in this method during synthesis are given below Equations (16)–(21) [76].





### 7.3. LaMer and Dinegar Model

The uniform dispersion of these synthesized particles is the priority for all applications and their subsequent results. The growth of monodispersed and uniform-sized metal-oxide (e.g., Fe-O) NP from their precursors depends upon the specific conditions, which remained without changing for a longer time. For more detailed understanding and justification, mostly two models explain this phenomenon and mechanism for completion of the growth of nuclei. The classic model, LaMer and Dinegar mechanism for growth into three stages, as shown in Figure 8, (I) the diffusion of monomers concentration gradually increases up to a specific supersaturation concentration essential for nucleation. (II) after supersaturation, a burst of nucleation occurs in which the solute diffuses from the solution for growth. (III) this growth proceeds by adding the monomer to the particle surface until the monodisperse final size particle is gained [77,78].

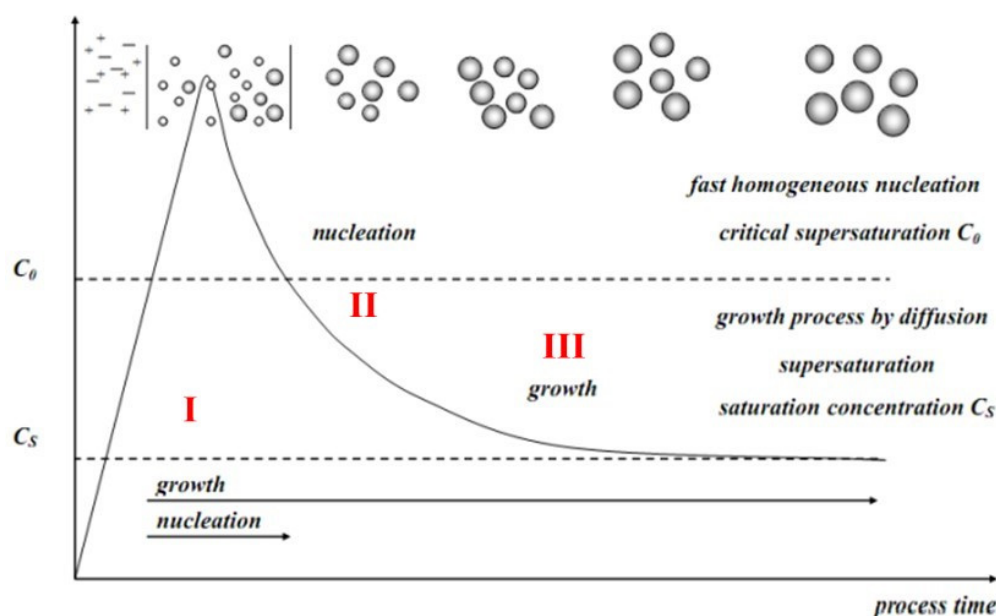


**Figure 8.** LaMer and Dinegar mechanism for monodisperse nanoparticles growth Adapted with permission from [78]. Copyright, 2016 American Chemical Society.

## 8. General Applications of Magnetite ( $\text{Fe}_3\text{O}_4$ )

Two kinds of iron oxides are magnetic in nature (i) magnetite ( $\text{Fe}_3\text{O}_4$ ) and (ii) maghemite ( $\text{Fe}_2\text{O}_3$ ,  $\gamma\text{-Fe}_2\text{O}_3$ ). These magnetic particles are different regarding the composition of iron, oxygen and grown under different conditions. Both are magnetic and extensively used in various kinds of applications. In addition, magnetite magnetic nanoparticles ( $\text{Fe}_3\text{O}_4$  NP) are receiving more interest from researchers due to the wide range of their application in numerous fields. The magnetic response is responsible for multifunctional applications in various sectors including energy storage, carbon capture, medical treatment, enzyme control, hydrogen storage, optical applications, nano electronics, and environmental remediation, as shown in Figure 9 [79–81]. These applications include utilization in the medical field such as for drug delivery, magnetic resonance imaging (MRI), and environmental treatments such as the removal of pollutants or contaminant particles [7]. Herein,  $\text{Fe}_3\text{O}_4$  is employed for the treatment of flue gas due to its distinguished magnetic and stability characteristic [82,83].

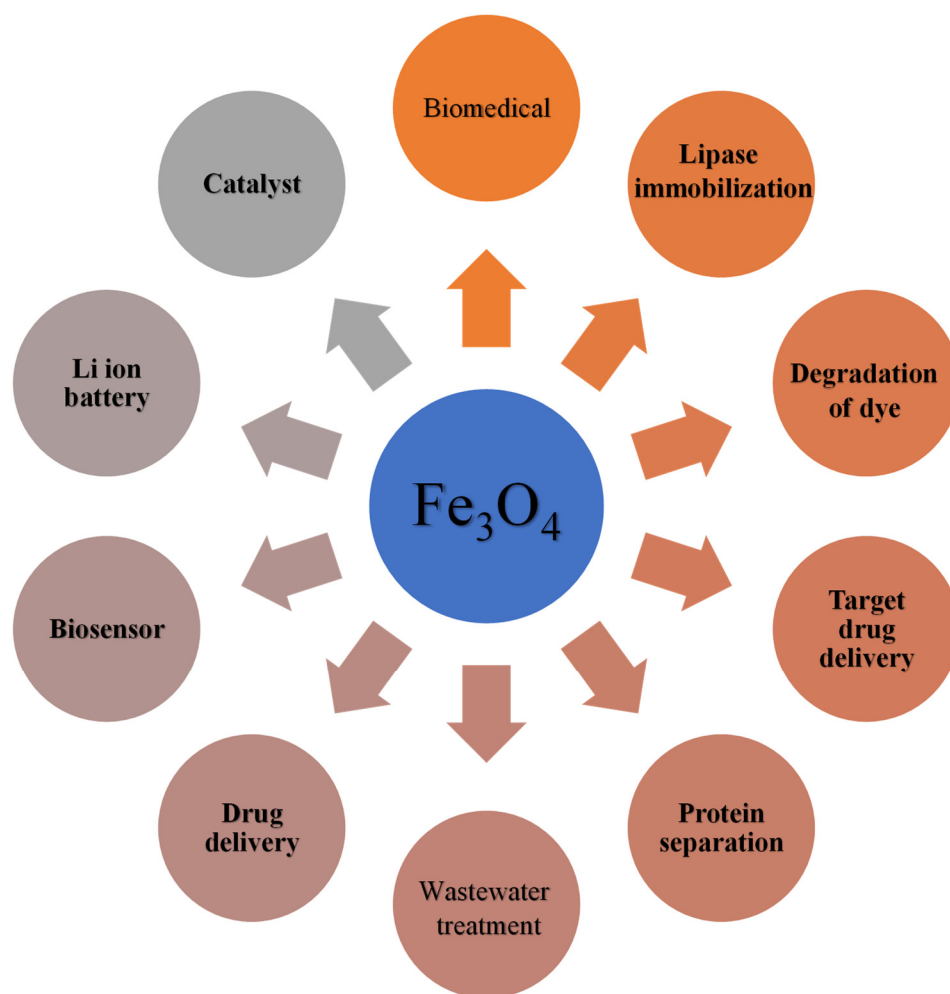


**Figure 9.** Applications of magnetite in various fields. Adapted with permission from [80]. Copyright, 2019 Springer.

Moreover, there are several other applications in which magnetic  $\text{Fe}_3\text{O}_4$  NP is directly used, such as in loudspeakers, for damping and cooling agents, low friction seals, the active magnetic membrane used for biological reactor and microfluidic flow [84].

## 9. Functionalization of Magnetite NP

The predominant and outstanding characteristic of the  $\text{Fe}_3\text{O}_4$  NP, which distinguished these NP over the other nanomaterials, is its magnetic property. Taking advantage of  $\text{Fe}_3\text{O}_4$  NP, these are used in numerous fields by functionalization or coating of different materials with it [85,86]. The functionalization of  $\text{Fe}_3\text{O}_4$  is very useful and makes for unique application in various fields and in the environment. This surface functionalization imparts characteristic properties, enhances stabilization, dispersion, interaction between the NP and target place, and stability over a long range of pH and temperature. The surface coating also avoids leaching, dissolution, aggregation, dispersion, surface charge exchange, increased surface area, porosity, and adsorption characterizations [75,87]. These unique characteristics make the material more functional, useful, and environmentally friendly.

### 9.1. Functionalized Magnetic NP for $\text{NO}_x$ and $\text{SO}_x$ Removal

A number of ways have been applied to make  $\text{Fe}_3\text{O}_4$  useful for various fields, including drug and gene transportation, magnetic resonance imaging (MRI), filtration and purification, wastewater and atmospheric treatment purposes [74,82]. Additionally, the magnetism is distinguished property, making these particles more promising for the en-

vironment. Taking advantage of magnetically fast separation and easy recycling ability without a mechanical loss for several cycles made them more suitable for low operational cost and long-lasting adsorbents [74,88,89]. Recently,  $\text{Fe}(\text{OH})_3$  and  $\text{Fe}_2\text{O}_3$  catalysts for the selective catalytic reduction of  $\text{NO}_x$  with  $\text{NH}_3$  ( $\text{NH}_3$ -SCR) were synthesized using a precipitation method and, subsequently, sulfated; the enhancing effect of  $\text{SO}_4^{2-}$  functionalization on the performance of  $\text{Fe}_2\text{O}_3$  catalyst in  $\text{NH}_3$ -SCR was then examined. Results show that when compared to unmodified  $\text{Fe}_2\text{O}_3$ , the  $\text{SO}_4^{2-}$ -functionalized  $\text{Fe}_2\text{O}_3$  catalysts had much higher SCR activity than non-treated  $\text{Fe}_2\text{O}_3$  catalysts. In particular, the  $\text{SO}_4^{2-}/\text{Fe}(\text{OH})_3$  catalyst demonstrates exceptional performance in  $\text{NH}_3$ -SCR, with  $\text{NO}_x$  conversion rates of more than 80% at temperatures ranging from 250 to 450 °C; in addition, it exhibits good catalytic stability and resistance to  $\text{H}_2\text{O} + \text{SO}_2$  in the presence of  $\text{NH}_3$ . In addition, the functionalization of  $\text{Fe}_2\text{O}_3$  NP by sulfuric acid inhibits its further growth and  $\text{SO}_4^{2-}$  ions combined with  $\text{Fe}^{3+}$  to form a stable sulphate complex. Actually, it increases the active-sites and the acid strength, which can inhibit the ammonia over-oxidation on  $\text{Fe}_2\text{O}_3$  and improve the  $\text{NO}_x$  performance of  $\text{Fe}_2\text{O}_3$  [90,91]. According to another study, improving the low-temperature  $\text{SO}_4^{2-}$ -tolerant selective catalytic reduction (SCR) of  $\text{NO}_x$  with  $\text{NH}_3$  is an intractable problem due to the difficulty of decomposing accumulated sulphates below 300 °C [92,93]. Moreover, the wide range of surface modification on the magnetic support offers more specific and efficient catalysts. After surface modification,  $\text{Fe}_3\text{O}_4$  is widely used for  $\text{NO}_x$ ,  $\text{SO}_x$  removal and reduction, while a few examples of these kinds of materials are enlisted in Table 5.

**Table 5.** Functionalization of  $\text{Fe}_3\text{O}_4$  by different organic/inorganic layers used for  $\text{NO}_x$  removal and  $\text{NO}_x$  reduction under different systems.

System/Material	Purpose	Reductant/Name of Technique	Year	Ref.
$\text{Fe}_3\text{O}_4$ -Chitosan	$\text{NO}_x$ removal	$\text{C}_6\text{H}_{12}\text{O}_6$ , microorganisms (Biological reduction)	2012	[94]
$\text{Fe}_3\text{O}_4$ -poly(styrene-glycidylmethacrylate)	$\text{NO}_x$ removal	By microorganisms (Biological reduction)	2013	[95]
$\text{Fe}_3\text{O}_4$	De- $\text{NO}_x$	SCR	2010	[96]
$\text{Fe}_3\text{O}_4/\text{rGO}$	$\text{NO}_x$ -sensing	Injection of NO in reacting chamber	2016	[97]
$\text{Fe}_3\text{O}_4/\text{mpg-C}_3\text{N}_4$	$\text{NO}_x$ oxidation and storage	Photocatalytic oxidation under visible light	2019	[98]
$\text{Fe}_3\text{O}_4\text{-TiO}_2$	$\text{NO}_x$ removal	Adsorption fixed-bed reactor and High temperature	2016	[99]
$\text{Fe}_3\text{O}_4$ and $\text{Fe}_2\text{O}_3$	De- $\text{NO}_x$	SCR by $\text{NH}_3$	2009	[100]
Rod-Shaped $\text{Fe}_2\text{O}_3$	$\text{NO}_x$ reduction	SCR by $\text{NH}_3$	2012	[101]
$\text{Fe}_3\text{O}_4@\text{CuS}$	Hg capture (Flue gas treatment)	Adsorption fixed-bed reactor	2018	[102]

### 9.2. Surface Modification of NP by Ligands

The surface modification depends upon the stability of the loaded-layer and its application under specific conditions. The metal organic ligands (M-L) are relatively more stable after loading on  $\text{Fe}_3\text{O}_4$  NP. A very common example of M-L is Ethylenediaminetetraacetic acid (EDTA) and Fe, extensively used for  $\text{NO}_x$  scrubbing treatment [103,104]. Although, this M-L system has been used for gas treatment for the last three decades. However, some very critical factors inhibit the industrial applications of EDTA-Fe for flue gas treatment. Those factors can be avoided if this EDTA-Fe load on the surface of  $\text{Fe}_3\text{O}_4$  achieves this, then, the liquid system is transformed into a solid system. Moreover, previous studies also

indicated the  $\text{Fe}_3\text{O}_4@EDTA$  system is very stable and showed high reusability [105,106]. The multi chelating ends (amino and carboxylic) of EDTA anchored the  $\text{Fe}_3\text{O}_4$  solid NP and positively charged metal ions ( $\text{Fe}^{\text{III/II}}$ ) by improving the overall stability and catalytic properties and the proposed general structure is shown in Figure 10 [107,108]. The EDTA further provides stability to the developed system due to its high stability over long-range of pH and potential of making metal-complexes without reduction [109,110]. Hence, the  $\text{Fe}_3\text{O}_4@EDTA\text{-Fe}$  is expected to be an ideal catalyst regarding stability, synergistic efficiency, and reusability.

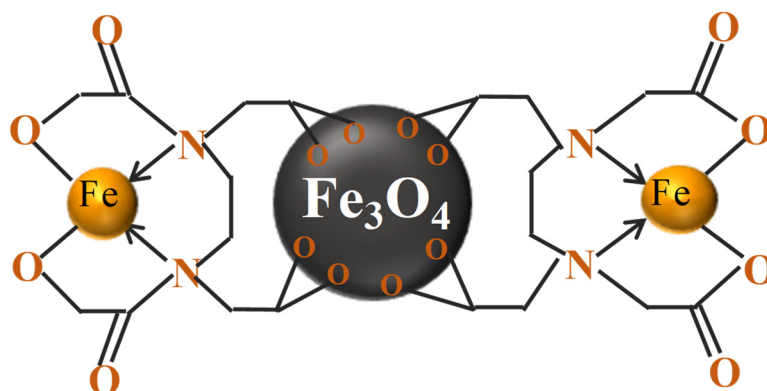


Figure 10. Proposed general structure of  $\text{Fe}_3\text{O}_4@EDTA\text{-Fe}$ .

## 10. Conclusions

Overall, the removal of  $\text{NO}_x$  and  $\text{SO}_2$  from the atmosphere offers significant promise for commercialization on a wide scale for various applications. This study discovered that wet scrubbing is an effective approach that can be used in mild conditions and has a low operational cost due to the ease with which it can be set up. These are the main advantages of this technique, according to the findings. Nevertheless, the need for a substantial amount of freshwater and the need to regenerate the catalyst or scrubbing solution are the primary obstacles to its widespread deployment. To meet the requirements of environmental protection organizations, various methods for the treatment of  $\text{NO}_x$ ,  $\text{SO}_2$ , and other pollutants have been devised and implemented at the individual industrial level. Some strategies are used to reduce  $\text{NO}_x$  production during combustion, while others reduce post-combustion  $\text{NO}_x$ . Dry sorbent injection (DSI), selective noncatalytic reduction (SNCR), wet flue gas desulfurization (FGD), and selective catalytic reduction (SCR) are some of the treatment options available (SCR). FGD and SCR were determined to be the most often employed methods for treating  $\text{NO}_x$  and  $\text{SO}_2$ , concurrently.  $\text{N}_2\text{O}$  cannot be recovered using this wet scrubbing method since the absorption and reduction occur under the same conditions (in particular, pH). Another major issue is that the solubility of  $\text{N}_2\text{O}$  in water is five times that of  $\text{NO}$  gas, making the separation of  $\text{N}_2\text{O}$  a difficult operation. It is a stable greenhouse gas (GHG) that causes various difficulties when emitted by  $\text{NO}_x$  treatment plants.  $\text{N}_2\text{O}$  is produced by tail gas, a severe concern because it is a greenhouse gas (GHG) that causes serious difficulties such as ozone depletion (ODS). To address these challenges, solvothermal production of solid magnetic nanomaterials such as iron-oxide nanoparticles and conducting functionalization of magnetite NP and surface modification of NP by ligands were used. It was also discovered that using various wet-scrubbing processes, the synthesis of solid iron-oxides such as magnetic ( $\text{Fe}_3\text{O}_4$ ) NP is gaining popularity among researchers due to the vast range of applications in a variety of sectors. Furthermore, EDTA coatings on  $\text{Fe}_3\text{O}_4$  NPs are commonly used because of their great stability over a wide pH range and their ability to form solid catalytic systems. Therefore, the  $\text{Fe}_3\text{O}_4@EDTA\text{-Fe}$  catalyst is expected to be the most stable, efficient, and reusable catalyst available in terms of stability, synergistic efficiency, and reusability. This review is beneficial for environmentalists, scientists, and specialists involved in minimizing

the detrimental impacts of NO<sub>x</sub> and SO<sub>2</sub> at academic and commercial levels in the research and development sectors.

**Author Contributions:** Conceptualization, writing—original draft preparation, datacuration M.A., I.H.; Review and editing-visualization, software and datacuration I.M., M.U., S.H.; Resources, editing and supervision H.M.A.S. All authors have read and agreed to the published version of the manuscript.

**Funding:** This study was supported by the National Natural Science Foundation of China (Grant No. 22050410268).

**Institutional Review Board Statement:** Not applicable.

**Informed Consent Statement:** Not applicable.

**Conflicts of Interest:** The authors declare no conflict of interest.

## References

1. Suchecki, T.; Kumazawa, H. Application of hydrazine to regeneration of post-absorption solutions in combined SO<sub>2</sub>/NO<sub>x</sub> removal from flue gases by a complex method. *Sep. Technol.* **1994**, *4*, 763–770.
2. Sharif, H.M.A.; Li, T.; Mahmood, N.; Ahmad, M.; Xu, J.; Mahmood, A.; Djellabi, R.; Yang, B. Thermally Activated Epoxy-functionalized Carbon as an Electrocatalyst for Efficient NO<sub>x</sub> Reduction. *Carbon* **2021**, *182*, 516–524. [[CrossRef](#)]
3. Manconi, I.; van der Maas, P.; Lens, P.N. Effect of sulfur compounds on biological reduction of nitric oxide in aqueous Fe(II)EDTA<sup>2-</sup> solutions. *Nitric Oxide* **2006**, *15*, 40–49. [[CrossRef](#)]
4. Raza, S.; Zhang, J.; Ali, I.; Li, X.; Liu, C. Recent trends in the development of biomass-based polymers from renewable resources and their environmental applications. *J. Taiwan Inst. Chem. Eng.* **2020**, *115*, 293–303. [[CrossRef](#)]
5. Ruth, L.A. Energy from municipal solid waste: A comparison with coal combustion technology. *Prog. Energy Combust. Sci.* **1998**, *24*, 545–564. [[CrossRef](#)]
6. Park, J.-H.; Ahn, J.-W.; Kim, K.-H.; Son, Y.-S. Historic and futuristic review of electron beam technology for the treatment of SO<sub>2</sub> and NO<sub>x</sub> in flue gas. *Chem. Eng. J.* **2019**, *355*, 351–366. [[CrossRef](#)]
7. Sharif, H.M.A.; Cheng, H.-Y.; Haider, M.R.; Khan, K.; Yang, L.; Wang, A.-J. NO Removal with Efficient Recovery of N<sub>2</sub>O by Using Recyclable Fe<sub>3</sub>O<sub>4</sub>@EDTA@Fe(II) Complex: A Novel Approach toward Resource Recovery from Flue Gas. *Environ. Sci. Technol.* **2018**, *53*, 1004–1013. [[CrossRef](#)]
8. Zhao, Y.; Hao, R.; Yuan, B.; Jiang, J. Simultaneous removal of SO<sub>2</sub>, NO and Hg<sup>0</sup> through an integrative process utilizing a cost-effective complex oxidant. *J. Hazard. Mater.* **2016**, *301*, 74–83. [[CrossRef](#)] [[PubMed](#)]
9. Rezaei, F.; Rownaghi, A.A.; Monjezi, S.; Lively, R.P.; Jones, C.W. SO<sub>x</sub>/NO<sub>x</sub> Removal from Flue Gas Streams by Solid Adsorbents: A Review of Current Challenges and Future Directions. *Energy Fuels* **2015**, *29*, 5467–5486. [[CrossRef](#)]
10. Sharif, H.M.A.; Farooq, M.; Hussain, I.; Ali, M.; Mujtaba, M.; Sultan, M.; Yang, B. Recent innovations for scaling up microbial fuel cell systems: Significance of physicochemical factors for electrodes and membranes materials. *J. Taiwan Inst. Chem. Eng.* **2021**, *129*, 207–226. [[CrossRef](#)]
11. Hussain, I.; Jalil, A.; Fatah, N.; Hamid, M.; Ibrahim, M.; Aziz, M.; Setiabudi, H. A highly competitive system for CO methanation over an active metal-free fibrous silica mordenite via in-situ ESR and FTIR studies. *Energy Convers. Manag.* **2020**, *211*, 112754. [[CrossRef](#)]
12. Ramachandran, B.; Herman, R.G.; Choi, S.; Stenger, H.G.; Lyman, C.E.; Sale, J.W. Testing zeolite SCR catalysts under protocol conditions for NO<sub>x</sub> abatement from stationary emission sources. *Catal. Today* **2000**, *55*, 281–290. [[CrossRef](#)]
13. Sims, R.E.; Rogner, H.-H.; Gregory, K. Carbon emission and mitigation cost comparisons between fossil fuel, nuclear and renewable energy resources for electricity generation. *Energy Policy* **2003**, *31*, 1315–1326. [[CrossRef](#)]
14. Hussain, I.; Jalil, A.; Hamid, M.; Hassan, N. Recent advances in catalytic systems in the prism of physicochemical properties to remediate toxic CO pollutants: A state-of-the-art review. *Chemosphere* **2021**, *277*, 130285. [[CrossRef](#)]
15. Richter, A.; Burrows, J.P.; Nüss, H.; Granier, C.; Niemeier, U. Increase in tropospheric nitrogen dioxide over China observed from space. *Nat. Cell Biol.* **2005**, *437*, 129–132. [[CrossRef](#)]
16. Guo, Q.; He, Y.; Sun, T.; Wang, Y.; Jia, J. Simultaneous removal of NO<sub>x</sub> and SO<sub>2</sub> from flue gas using combined Na<sub>2</sub>SO<sub>3</sub> assisted electrochemical reduction and direct electrochemical reduction. *J. Hazard. Mater.* **2014**, *276*, 371–376. [[CrossRef](#)]
17. Zhang, R.; Wang, G.; Guo, S.; Zamora, M.L.; Ying, Q.; Lin, Y.; Wang, W.; Hu, M.; Wang, Y. Formation of Urban Fine Particulate Matter. *Chem. Rev.* **2015**, *115*, 3803–3855. [[CrossRef](#)] [[PubMed](#)]
18. Nakatsuji, T.; Yasukawa, R.; Tabata, K.; Ueda, K.; Niwa, M. A highly durable catalytic NO<sub>x</sub> reduction in the presence of SO<sub>x</sub> using periodic two steps, an operation in oxidizing conditions and a relatively short operation in reducing conditions. *Appl. Catal. B Environ.* **1999**, *21*, 121–131. [[CrossRef](#)]
19. Muzio, L.; Quartucy, G. Implementing NO<sub>x</sub> control: Research to application. *Prog. Energy Combust. Sci.* **1997**, *23*, 233–266. [[CrossRef](#)]



20. Sharif, H.M.A.; Mahmood, A.; Djellabi, R.; Cheng, H.-Y.; Dong, H.; Ajibade, F.O.; Ali, I.; Yang, B.; Wang, A.-J. Utilization of electrochemical treatment and surface reconstruction to achieve long lasting catalyst for NO<sub>x</sub> removal. *J. Hazard. Mater.* **2021**, *401*, 123440. [[CrossRef](#)]
21. Shi, K.; Liang, B.; Guo, Q.; Zhao, Y.; Sharif, H.M.A.; Li, Z.; Chen, E.; Wang, A. Accelerated bioremediation of a complexly contaminated river sediment through ZVI-electrode combined stimulation. *J. Hazard. Mater.* **2021**, *413*, 125392. [[CrossRef](#)]
22. Skalska, K.; Miller, J.S.; Ledakowicz, S. Trends in NO<sub>x</sub> abatement: A review. *Sci. Total Environ.* **2010**, *408*, 3976–3989. [[CrossRef](#)]
23. Dora, J.; Gostomczyk, M.A.; Jakubiak, M.; Kordylewski, W.; Mista, W.; Tkaczuk, M. Parametric studies of the effectiveness of NO oxidation process by ozone. *Chem. Process Eng.* **2009**, *30*, 621–634.
24. Pasel, J.; Káľšner, P.; Montanari, B.; Gazzano, M.; Vaccari, A.; Makowski, W.; Lojewski, T.; Dziembaj, R.; Papp, H. Transition metal oxides supported on active carbons as low temperature catalysts for the selective catalytic reduction (SCR) of NO with NH<sub>3</sub>. *Appl. Catal. B Environ.* **1998**, *18*, 199–213. [[CrossRef](#)]
25. Gómez-García, M.A.; Pitchon, V.; Kiennemann, A. Pollution by nitrogen oxides: An approach to NO<sub>x</sub> abatement by using sorbing catalytic materials. *Environ. Int.* **2005**, *31*, 445–467. [[CrossRef](#)]
26. Nakajima, F.; Hamada, I. The state-of-the-art technology of NO<sub>x</sub> control. *Catal. Today* **1996**, *29*, 109–115. [[CrossRef](#)]
27. Hussain, I.; Jalil, A.A.; Hassan, N.S.; Farooq, M.; Mujtaba, M.A.; Hamid, M.Y.S.; Sharif, H.M.A.; Nabgan, W.; Aziz, M.A.H.; Owgi, A.H.K. Contemporary thrust and emerging prospects of catalytic systems for substitute natural gas production by CO methanation. *Fuel* **2021**, 122604. [[CrossRef](#)]
28. Murayama, T.; Chen, J.; Hirata, J.; Matsumoto, K.; Ueda, W. Hydrothermal synthesis of octahedra-based layered niobium oxide and its catalytic activity as a solid acid. *Catal. Sci. Technol.* **2014**, *4*, 4250–4257. [[CrossRef](#)]
29. Okazaki, S.; Kuroha, H.; Okuyama, T. Effect of Nb<sub>2</sub>O<sub>5</sub> addition on the Catalytic Activity of Fe<sub>2</sub>O<sub>3</sub> for Reduction of NO<sub>x</sub> with NH<sub>3</sub> and O<sub>2</sub>. *Chem. Lett.* **1985**, *14*, 45–48. [[CrossRef](#)]
30. Ma, Z.; Wu, X.; Si, Z.; Weng, D.; Ma, J.; Xu, T. Impacts of niobia loading on active sites and surface acidity in NbO<sub>x</sub>/CeO<sub>2</sub>-ZrO<sub>2</sub> NH<sub>3</sub>-SCR catalysts. *Appl. Catal. B Environ.* **2015**, *179*, 380–394. [[CrossRef](#)]
31. Mosrati, J.; Atia, H.; Eckelt, R.; Lund, H.; Agostini, G.; Bentrup, U.; Rockstroh, N.; Keller, S.; Armbruster, U.; Mhamdi, M. Nb-Modified Ce/Ti Oxide Catalyst for the Selective Catalytic Reduction of NO with NH<sub>3</sub> at Low Temperature. *Catalysts* **2018**, *8*, 175. [[CrossRef](#)]
32. Li, W.; Guo, R.-T.; Wang, S.-X.; Pan, W.-G.; Chen, Q.-L.; Li, M.-Y.; Sun, P.; Liu, S.-M. The enhanced Zn resistance of Mn/TiO<sub>2</sub> catalyst for NH<sub>3</sub>-SCR reaction by the modification with Nb. *Fuel Process. Technol.* **2016**, *154*, 235–242. [[CrossRef](#)]
33. Lian, Z.; Liu, F.; He, H.; Shi, X.; Mo, J.; Wu, Z. Manganese–niobium mixed oxide catalyst for the selective catalytic reduction of NO<sub>x</sub> with NH<sub>3</sub> at low temperatures. *Chem. Eng. J.* **2014**, *250*, 390–398. [[CrossRef](#)]
34. Javed, M.T.; Irfan, N.; Gibbs, B. Control of combustion-generated nitrogen oxides by selective non-catalytic reduction. *J. Environ. Manag.* **2007**, *83*, 251–289. [[CrossRef](#)]
35. Sharif, H.M.A.; Mahmood, N.; Wang, S.; Hussain, I.; Hou, Y.-N.; Yang, L.-H.; Zhao, X.; Yang, B. Recent advances in hybrid wet scrubbing techniques for NO<sub>x</sub> and SO<sub>2</sub> removal: State of the art and future research. *Chemosphere* **2021**, *273*, 129695. [[CrossRef](#)]
36. Miller, B.G. *Coal Energy Systems*; Academic Press: Burlington, MA, USA, 2005.
37. Krum, K.R.K.; Jensen, M.; Li, S.; Norman, T.; Marshall, P.; Wu, H.; Glarborg, P. Selective Noncatalytic Reduction of NO<sub>x</sub> Using Ammonium Sulfate. *Energy Fuels* **2021**, *35*, 12392–12402. [[CrossRef](#)]
38. Han, L.; Cai, S.; Gao, M.; Hasegawa, J.-Y.; Wang, P.; Zhang, J.; Shi, L.; Zhang, D. Selective Catalytic Reduction of NO<sub>x</sub> with NH<sub>3</sub> by Using Novel Catalysts: State of the Art and Future Prospects. *Chem. Rev.* **2019**, *119*, 10916–10976. [[CrossRef](#)]
39. Chien, T.-W.; Chu, H. Removal of SO<sub>2</sub> and NO from flue gas by wet scrubbing using an aqueous NaClO<sub>2</sub> solution. *J. Hazard. Mater.* **2000**, *80*, 43–57. [[CrossRef](#)]
40. Wang, L.; Zhao, W.; Wu, Z. Simultaneous absorption of NO and SO<sub>2</sub> by Fe(II)EDTA combined with Na<sub>2</sub>SO<sub>3</sub> solution. *Chem. Eng. J.* **2007**, *132*, 227–232. [[CrossRef](#)]
41. Wang, H.; Chen, H.; Wang, Y.; Lyu, Y.-K. Performance and mechanism comparison of manganese oxides at different valence states for catalytic oxidation of NO. *Chem. Eng. J.* **2019**, *361*, 1161–1172. [[CrossRef](#)]
42. Jin, D.-S.; Deshwal, B.-R.; Park, Y.-S.; Lee, H.-K. Simultaneous removal of SO<sub>2</sub> and NO by wet scrubbing using aqueous chlorine dioxide solution. *J. Hazard. Mater.* **2006**, *135*, 412–417. [[CrossRef](#)]
43. Gao, F.; Tang, X.; Yi, H.; Zhao, S.; Li, C.; Li, J.; Shi, Y.; Meng, X. A Review on Selective Catalytic Reduction of NO<sub>x</sub> by NH<sub>3</sub> over Mn-Based Catalysts at Low Temperatures: Catalysts, Mechanisms, Kinetics and DFT Calculations. *Catalysts* **2017**, *7*, 199. [[CrossRef](#)]
44. McKinlay, A.C.; Eubank, J.F.; Wuttke, S.; Xiao, B.; Wheatley, P.S.; Bazin, P.; LaValley, J.-C.; Daturi, M.; Vimont, A.; De Weireld, G.; et al. Nitric Oxide Adsorption and Delivery in Flexible MIL-88(Fe) Metal–Organic Frameworks. *Chem. Mater.* **2013**, *25*, 1592–1599. [[CrossRef](#)]
45. Ma, C.; Yi, H.; Tang, X.; Zhao, S.; Yang, K.; Song, L.; Zhang, Y.; Wang, Y. Improving simultaneous removal efficiency of SO<sub>2</sub> and NO<sub>x</sub> from flue gas by surface modification of MgO with organic component. *J. Clean. Prod.* **2019**, *230*, 508–517. [[CrossRef](#)]
46. Zhao, C.; Chen, X.; Zhao, C. CO<sub>2</sub> Absorption Using Dry Potassium-Based Sorbents with Different Supports. *Energy Fuels* **2009**, *23*, 4683–4687. [[CrossRef](#)]
47. Chang, J.C.S.; Kaplan, N. SO<sub>2</sub> removal by limestone dual alkali. *Environ. Prog.* **1984**, *3*, 267–274. [[CrossRef](#)]

48. Barman, S.; Philip, L. Integrated System for the Treatment of Oxides of Nitrogen from Flue Gases. *Environ. Sci. Technol.* **2006**, *40*, 1035–1041. [[CrossRef](#)]
49. Koh, H.K.; Geller, A.C.; VanderWeele, T.J. Deaths from COVID-19. *JAMA* **2021**, *325*, 133–134. [[CrossRef](#)] [[PubMed](#)]
50. Zhang, X.; Zhang, X.; Yang, X.; Chen, Y.; Hu, X.; Wu, X. CeMn/TiO<sub>2</sub> catalysts prepared by different methods for enhanced low-temperature NH<sub>3</sub>-SCR catalytic performance. *Chem. Eng. Sci.* **2021**, *238*, 116588. [[CrossRef](#)]
51. Djellabi, R.; Yang, B.; Xiao, K.; Gong, Y.; Cao, D.; Sharif, H.M.A.; Zhao, X.; Zhu, C.; Zhang, J. Unravelling the mechanistic role of Ti-O-C bonding bridge at titania/lignocellulosic biomass interface for Cr(VI) photoreduction under visible light. *J. Colloid Interface Sci.* **2019**, *553*, 409–417. [[CrossRef](#)] [[PubMed](#)]
52. Guan, J.; Zhou, L.; Li, W.; Hu, D.; Wen, J.; Huang, B. Improving the Performance of Gd Addition on Catalytic Activity and SO<sub>2</sub> Resistance over MnOx/ZSM-5 Catalysts for Low-Temperature NH<sub>3</sub>-SCR. *Catalysts* **2021**, *11*, 324. [[CrossRef](#)]
53. Cooper, C.E. Nitric oxide and iron proteins. *Biochim. Biophys. Acta (BBA)-Bioenerg.* **1999**, *1411*, 290–309. [[CrossRef](#)]
54. Sada, E.; Kumazawa, H.; Machida, H. Absorption of dilute NO into aqueous solutions of Na<sub>2</sub>SO<sub>3</sub> with added Fe(II)NTA and reduction kinetics of Fe(III)NTA by Na<sub>2</sub>SO. *Ind. Eng. Chem. Res.* **1987**, *26*, 2016–2019. [[CrossRef](#)]
55. Littlejohn, D.; Chang, S.G. Reaction of ferrous chelate nitrosyl complexes with sulfite and bisulfite ions. *Ind. Eng. Chem. Res.* **1990**, *29*, 10–14. [[CrossRef](#)]
56. van der Maas, P.; Peng, S.; Klapwijk, B.; Lens, P. Enzymatic versus Nonenzymatic Conversions during the Reduction of EDTA-Chelated Fe(III) in BioDeNOx Reactors. *Environ. Sci. Technol.* **2005**, *39*, 2616–2623. [[CrossRef](#)] [[PubMed](#)]
57. Ma, J.-F.; Hou, Y.-N.; Guo, J.; Sharif, H.M.A.; Huang, C.; Zhao, J.; Li, H.; Song, Y.; Lu, C.; Han, Y.; et al. Rational design of biogenic PdAu nanoparticles with enhanced catalytic performance for electrocatalysis and azo dyes degradation. *Environ. Res.* **2022**, *204*, 112086. [[CrossRef](#)]
58. Xia, Y.; Zhao, J.; Li, M.; Zhang, S.; Li, S.; Li, W. Bioelectrochemical Reduction of Fe(II)EDTA–NO in a Biofilm Electrode Reactor: Performance, Mechanism, and Kinetics. *Environ. Sci. Technol.* **2016**, *50*, 3846–3851. [[CrossRef](#)] [[PubMed](#)]
59. Mendelsohn, M.H.; Harkness, J.B.L. Enhanced flue-gas denitrification using ferrous.cntdot.EDTA and a polyphenolic compound in an aqueous scrubber system. *Energy Fuels* **1991**, *5*, 244–248. [[CrossRef](#)]
60. Sada, E.; Kumazawa, H.; Takada, Y. Chemical reactions accompanying absorption of nitric oxide into aqueous mixed solutions of iron(II)-EDTA and sodium sulfite. *Ind. Eng. Chem. Fundam.* **1984**, *23*, 60–64. [[CrossRef](#)]
61. Buisman, C.J.N.; Dijkman, H.; Verbraak, P.L.; Den Hartog, A.J. Process for Purifying Flue Gas Containing Nitrogen Oxides. U.S. Patent 5,891,408, 6 April 1999.
62. Sada, E.; Kumazawa, H.; Kudo, I.; Kondo, T. Individual and Simultaneous Absorption of Dilute NO and SO<sub>2</sub> in Aqueous Slurries of MgSO<sub>3</sub> with FeII-EDTA. *Ind. Eng. Chem. Process. Des. Dev.* **1980**, *19*, 377–382. [[CrossRef](#)]
63. Maas, P.V.D.; Van de Sandt, T.; Klapwijk, B.; Lens, P. Biological reduction of nitric oxide in aqueous Fe (II) EDTA solutions. *Biotechnol. Prog.* **2003**, *19*, 1323–1328. [[CrossRef](#)] [[PubMed](#)]
64. Zhang, S.; Cai, L.-L.; Mi, X.-H.; Jiang, J.-L.; Li, W. NO<sub>x</sub>Removal from Simulated Flue Gas by Chemical Absorption–Biological Reduction Integrated Approach in a Biofilter. *Environ. Sci. Technol.* **2008**, *42*, 3814–3820. [[CrossRef](#)]
65. Mahmood, A. Photovoltaic and Charge Transport Behavior of Diketopyrrolopyrrole Based Compounds with A–D–A–D–A Skeleton. *J. Clust. Sci.* **2019**, *30*, 1123–1130. [[CrossRef](#)]
66. Suchecki, T.T.; Mathews, B.; Kumazawa, H. Kinetic Study of Ambient-Temperature Reduction of FeIIiedta by Na<sub>2</sub>S<sub>2</sub>O. *Ind. Eng. Chem. Res.* **2005**, *44*, 4249–4253. [[CrossRef](#)]
67. Mok, Y.S.; Lee, H.-J. Removal of sulfur dioxide and nitrogen oxides by using ozone injection and absorption–reduction technique. *Fuel Process. Technol.* **2006**, *87*, 591–597. [[CrossRef](#)]
68. Mogili, P.; Kleiber, P.; Young, M.; Grassian, V. N<sub>2</sub>O<sub>5</sub> hydrolysis on the components of mineral dust and sea salt aerosol: Comparison study in an environmental aerosol reaction chamber. *Atmos. Environ.* **2006**, *40*, 7401–7408. [[CrossRef](#)]
69. Daniel, A.L.; Dilip, R. Ahuja. Relative contributions of greenhouse gas emissions to global warming. *Nature* **1990**, *344*, 529–531.
70. Usman, M.; Byrne, J.; Chaudhary, A.; Orsetti, S.; Hanna, K.; Ruby, C.; Kappler, A.; Haderlein, S.B. Magnetite and Green Rust: Synthesis, Properties, and Environmental Applications of Mixed-Valent Iron Minerals. *Chem. Rev.* **2018**, *118*, 3251–3304. [[CrossRef](#)]
71. Kong, L.; Lu, X.; Bian, X.; Zhang, W.; Wang, C. Constructing Carbon-Coated Fe<sub>3</sub>O<sub>4</sub> Microspheres as Antacid and Magnetic Support for Palladium Nanoparticles for Catalytic Applications. *ACS Appl. Mater. Interfaces* **2011**, *3*, 35–42. [[CrossRef](#)]
72. Ali, I.; Li, J.; Peng, C.; Qasim, M.; Khan, Z.M.; Naz, I.; Sultan, M.; Rauf, M.; Iqbal, W.; Sharif, H.M.A. 3-Dimensional membrane capsules: Synthesis modulations for the remediation of environmental pollutants—A critical review. *Crit. Rev. Environ. Sci. Technol.* **2020**, *10*, 1–62. [[CrossRef](#)]
73. Ali, A.; Zafar, H.; Zia, M.; ul Haq, I.; Phull, A.R.; Ali, J.S.; Hussain, A. Synthesis, characterization, applications, and challenges of iron oxide nanoparticles. *Nanotechnol. Sci. Appl.* **2016**, *9*, 49–67. [[CrossRef](#)] [[PubMed](#)]
74. Zhu, M.; Wang, C.; Meng, D.; Diao, G. In situ synthesis of silver nanostructures on magnetic Fe<sub>3</sub>O<sub>4</sub>@C core–shell nanocomposites and their application in catalytic reduction reactions. *J. Mater. Chem. A* **2013**, *1*, 2118–2125. [[CrossRef](#)]
75. Zhao, N.; Yan, L.; Zhao, X.; Chen, X.; Li, A.; Zheng, D.; Zhou, X.; Dai, X.; Xu, F.-J. Versatile Types of Organic/Inorganic Nanohybrids: From Strategic Design to Biomedical Applications. *Chem. Rev.* **2019**, *119*, 1666–1762. [[CrossRef](#)] [[PubMed](#)]
76. Palchoudhury, S.; An, W.; Xu, Y.; Qin, Y.; Zhang, Z.; Chopra, N.; Holler, R.A.; Turner, C.H.; Bao, Y. Synthesis and Growth Mechanism of Iron Oxide Nanowhiskers. *Nano Lett.* **2011**, *11*, 1141–1146. [[CrossRef](#)]

77. Vreeland, E.C.; Watt, J.; Schober, G.B.; Hance, B.G.; Austin, M.J.; Price, A.D.; Fellows, B.D.; Monson, T.C.; Hudak, N.S.; Maldonado-Camargo, L.; et al. Enhanced Nanoparticle Size Control by Extending LaMer's Mechanism. *Chem. Mater.* **2015**, *27*, 6059–6066. [[CrossRef](#)]
78. Wu, L.; Mendoza-Garcia, A.; Li, Q.; Sun, S. Organic Phase Syntheses of Magnetic Nanoparticles and Their Applications. *Chem. Rev.* **2016**, *116*, 10473–10512. [[CrossRef](#)]
79. Siddiqui, M.T.H.; Nizamuddin, S.; Baloch, H.A.; Mubarak, N.M.; Dumbre, D.K.; Inamuddin, A.A.M.; Bhutto, A.W.; Srinivasan, M.; Griffin, G.J. Synthesis of magnetic carbon nanocomposites by hydrothermal carbonization and pyrolysis. *Environ. Chem. Lett.* **2018**, *16*, 821–844. [[CrossRef](#)]
80. Devi, S.M.; Nivetha, A.; Prabha, I. Superparamagnetic Properties and Significant Applications of Iron Oxide Nanoparticles for Astonishing Efficacy—A Review. *J. Supercond. Nov. Magn.* **2019**, *32*, 127–144. [[CrossRef](#)]
81. Ali, J.; Wang, L.; Waseem, H.; Sharif, H.M.A.; Djellabi, R.; Zhang, C.; Pan, G. Bioelectrochemical recovery of silver from wastewater with sustainable power generation and its reuse for biofouling mitigation. *J. Clean. Prod.* **2019**, *235*, 1425–1437. [[CrossRef](#)]
82. Lu, A.-H.; Salabas, E.-L.; Schüth, F. Magnetic Nanoparticles: Synthesis, Protection, Functionalization, and Application. *Angew. Chem. Int. Ed.* **2007**, *46*, 1222–1244. [[CrossRef](#)]
83. Sharif, H.M.A.; Mahmood, A.; Cheng, H.-Y.; Djellabi, R.; Ali, J.; Jiang, W.-L.; Wang, S.-S.; Haider, M.R.; Mahmood, N.; Wang, A.-J. Fe<sub>3</sub>O<sub>4</sub> Nanoparticles Coated with EDTA and Ag Nanoparticles for the Catalytic Reduction of Organic Dyes from Wastewater. *ACS Appl. Nano Mater.* **2019**, *2*, 5310–5319. [[CrossRef](#)]
84. Yang, L.-H.; Cheng, H.-Y.; Ding, Y.-C.; Su, S.-G.; Wang, B.; Zeng, R.; Sharif, H.M.A.; Wang, A.-J. Enhanced treatment of coal gasification wastewater in a membraneless sleeve-type bioelectrochemical system. *Bioelectrochemistry* **2019**, *129*, 154–161. [[CrossRef](#)] [[PubMed](#)]
85. Liu, Y.; Chen, T.; Wu, C.; Qiu, L.; Hu, R.; Li, J.; Cansiz, S.; Zhang, L.; Cui, C.; Zhu, G.; et al. Facile Surface Functionalization of Hydrophobic Magnetic Nanoparticles. *J. Am. Chem. Soc.* **2014**, *136*, 12552–12555. [[CrossRef](#)] [[PubMed](#)]
86. Mahmood, A.; Wang, J.-L. Machine learning for high performance organic solar cells: Current scenario and future prospects. *Energy Environ. Sci.* **2021**, *14*, 90–105. [[CrossRef](#)]
87. Chaudhuri, R.; Paria, S. Core/Shell Nanoparticles: Classes, Properties, Synthesis Mechanisms, Characterization, and Applications. *Chem. Rev.* **2012**, *112*, 2373–2433. [[CrossRef](#)]
88. Zhang, Y.-X.; Yu, X.-Y.; Jin, Z.; Jia, Y.; Xu, W.-H.; Luo, T.; Zhu, B.-J.; Liu, J.-H.; Huang, X.-J. Ultra high adsorption capacity of fried egg jellyfish-like  $\gamma$ -AlOOH(Boehmite)@SiO<sub>2</sub>/Fe<sub>3</sub>O<sub>4</sub> porous magnetic microspheres for aqueous Pb(II) removal. *J. Mater. Chem.* **2011**, *21*, 16550–16557. [[CrossRef](#)]
89. Mahmood, A.; Wang, J.-L. A time and resource efficient machine learning assisted design of non-fullerene small molecule acceptors for P3HT-based organic solar cells and green solvent selection. *J. Mater. Chem. A* **2021**, *9*, 15684–15695. [[CrossRef](#)]
90. Wang, H.-M.; Ma, Y.-P.; Chen, X.-Y.; Xu, S.-Y.; Chen, J.-D.; Zhang, Q.-L.; Zhao, B.; Ning, P. Promoting effect of SO<sub>2</sub>-4 functionalization on the performance of Fe<sub>2</sub>O<sub>3</sub> catalyst in the selective catalytic reduction of NO<sub>x</sub> with NH<sub>3</sub>. *J. Fuel Chem. Technol.* **2020**, *48*, 584–593. [[CrossRef](#)]
91. Jia, L.; Yu, Y.; Li, Z.-p.; Qin, S.-n.; Guo, J.-r.; Zhang, Y.-q.; Wang, J.-c.; Zhang, J.-c.; Fan, B.-g.; Jin, Y. Study on the Hg<sup>0</sup> removal characteristics and synergistic mechanism of iron-based modified biochar doped with multiple metals. *Bioresour. Technol.* **2021**, *332*, 125086. [[CrossRef](#)]
92. Han, L.; Gao, M.; Hasegawa, J.-Y.; Li, S.; Shen, Y.; Li, H.; Shi, L.; Zhang, D. SO<sub>2</sub>-Tolerant Selective Catalytic Reduction of NO<sub>x</sub> over Meso-TiO<sub>2</sub>@Fe<sub>2</sub>O<sub>3</sub>@Al<sub>2</sub>O<sub>3</sub> Metal-Based Monolith Catalysts. *Environ. Sci. Technol.* **2019**, *53*, 6462–6473. [[CrossRef](#)]
93. Hu, Z.; Zhang, L.; Huang, J.; Feng, Z.; Xiong, Q.; Ye, Z.; Chen, Z.; Li, X.; Yu, Z. Self-supported nickel-doped molybdenum carbide nanoflower clusters on carbon fiber paper for an efficient hydrogen evolution reaction. *Nanoscale* **2021**, *13*, 8264–8274. [[CrossRef](#)]
94. Jing, G.; Zhou, J.; Zhou, Z.; Lin, T. Reduction of Fe(III)EDTA— in a NO<sub>x</sub> scrubbing solution by magnetic Fe<sub>3</sub>O<sub>4</sub>-chitosan microspheres immobilized mixed culture of iron-reducing bacteria. *Bioresour. Technol.* **2012**, *108*, 169–175. [[CrossRef](#)] [[PubMed](#)]
95. Wang, X.; Zhou, Z.; Jing, G. Synthesis of Fe<sub>3</sub>O<sub>4</sub> poly(styrene-glycidyl methacrylate) magnetic porous microspheres and application in the immobilization of Klebsiella sp. FD-3 to reduce Fe(III) EDTA in a NO<sub>x</sub> scrubbing solution. *Bioresour. Technol.* **2013**, *130*, 750–756. [[CrossRef](#)]
96. Yao, G.-H.; Gui, K.-T.; Wang, F. Low-Temperature De-NO<sub>x</sub> by Selective Catalytic Reduction Based on Iron-Based Catalysts. *Chem. Eng. Technol.* **2010**, *33*, 1093–1098. [[CrossRef](#)]
97. Yang, Y.; Sun, L.; Dong, X.; Yu, H.; Wang, T.; Wang, J.; Wang, R.; Yu, W.; Liu, G. Fe<sub>3</sub>O<sub>4</sub>/rGO nanocomposite: Synthesis and enhanced NO<sub>x</sub> gas-sensing properties at room temperature. *RSC Adv.* **2016**, *6*, 37085–37092. [[CrossRef](#)]
98. Irfan, M.; Sevim, M.; Koçak, Y.; Balci, M.; Metin, Ö.; Ozensoy, E. Enhanced Photocatalytic NO<sub>x</sub> Oxidation and Storage Under Visible-Light Irradiation by Anchoring Fe<sub>3</sub>O<sub>4</sub> Nanoparticles on Mesoporous Graphitic Carbon Nitride (mpg-C<sub>3</sub>N<sub>4</sub>). *Appl. Catal. B Environ.* **2019**, *249*, 126–137. [[CrossRef](#)]
99. Li, Y.; Yi, H.; Tang, X.; Liu, X.; Wang, Y.; Cui, B.; Zhao, S. Study on the performance of simultaneous desulfurization and denitrification of Fe<sub>3</sub>O<sub>4</sub>-TiO<sub>2</sub> composites. *Chem. Eng. J.* **2016**, *304*, 89–97. [[CrossRef](#)]
100. Santiago, R.; Mossin, S.; Bedia, J.; Fehrmann, R.; Palomar, J. Methanol-Promoted Oxidation of Nitrogen Oxide (NO<sub>x</sub>) by Encapsulated Ionic Liquids. *Environ. Sci. Technol.* **2019**, *53*, 11969–11978. [[CrossRef](#)]
101. Mou, X.; Zhang, B.; Li, Y.; Yao, L.; Wei, X.; Su, D.S.; Shen, W. Rod-Shaped Fe<sub>2</sub>O<sub>3</sub> as an Efficient Catalyst for the Selective Reduction of Nitrogen Oxide by Ammonia. *Angew. Chem. Int. Ed.* **2012**, *51*, 2989–2993. [[CrossRef](#)]

102. Yang, Z.; Li, H.; Liao, C.; Zhao, J.; Feng, S.; Li, P.; Liu, X.; Yang, J.; Shih, K. Magnetic Rattle-Type Fe<sub>3</sub>O<sub>4</sub>@CuS Nanoparticles as Recyclable Sorbents for Mercury Capture from Coal Combustion Flue Gas. *ACS Appl. Nano Mater.* **2018**, *1*, 4726–4736. [[CrossRef](#)]
103. van der Maas, P.; Brink, P.V.D.; Klapwijk, B.; Lens, P. Acceleration of the Fe(III)EDTA– reduction rate in BioDeNO<sub>x</sub> reactors by dosing electron mediating compounds. *Chemosphere* **2009**, *75*, 243–249. [[CrossRef](#)] [[PubMed](#)]
104. Zhang, X.; Tang, Y.; Zhang, F.; Lee, C.-S. A Novel Aluminum–Graphite Dual-Ion Battery. *Adv. Energy Mater.* **2016**, *6*, 1502588. [[CrossRef](#)]
105. Warner, C.L.; Addleman, R.S.; Cinson, A.D.; Droubay, T.C.; Engelhard, M.H.; Nash, M.A.; Yantasee, W.; Warner, M.G. High-Performance, Superparamagnetic, Nanoparticle-Based Heavy Metal Sorbents for Removal of Contaminants from Natural Waters. *ChemSusChem* **2010**, *3*, 749–757. [[CrossRef](#)] [[PubMed](#)]
106. Wang, P.; Wang, S.-Z.; Kang, Y.-R.; Sun, Z.-S.; Wang, X.-D.; Meng, Y.; Hong, M.-H.; Xie, W.-F. Cauliflower-shaped Bi<sub>2</sub>O<sub>3</sub>–ZnO heterojunction with superior sensing performance towards ethanol. *J. Alloy. Compd.* **2021**, *854*, 157152. [[CrossRef](#)]
107. Zhao, F.; Repo, E.; Yin, D.; Meng, Y.; Jafari, S.; Sillanpää, M. EDTA-cross-linked β-cyclodextrin: An environmentally friendly bifunctional adsorbent for simultaneous adsorption of metals and cationic dyes. *Environ. Sci. Technol.* **2015**, *49*, 10570–10580. [[CrossRef](#)]
108. Aghazadeh, M.; Karimzadeh, I.; Ganjali, M.R. Ethylenediaminetetraacetic acid capped superparamagnetic iron oxide (Fe<sub>3</sub>O<sub>4</sub>) nanoparticles: A novel preparation method and characterization. *J. Magn. Magn. Mater.* **2017**, *439*, 312–319. [[CrossRef](#)]
109. Kim, G.; Choi, W. Charge-transfer surface complex of EDTA-TiO<sub>2</sub> and its effect on photocatalysis under visible light. *Appl. Catal. B Environ.* **2010**, *100*, 77–83. [[CrossRef](#)]
110. Wang, G.; Tomasella, F.P. Ion-pairing HPLC methods to determine EDTA and DTPA in small molecule and biological pharmaceutical formulations. *J. Pharm. Anal.* **2016**, *6*, 150–156. [[CrossRef](#)]